

## Feature extraction of Jabon (*Anthocephalus sp*) leaf disease using discrete wavelet transform

Felliks Feiters Tampinongkol<sup>1</sup>, Yeni Herdiyeni<sup>2</sup>, Elis Nina Herliyana<sup>3</sup>

<sup>1,2</sup>Department of Computer Science, Bogor Agricultural University, Indonesia

<sup>3</sup>Department of Silviculture, Bogor Agricultural University, Indonesia

### Article Info

#### Article history:

Received Jul 31, 2019

Revised Jan 17, 2020

Accepted Feb 21, 2020

#### Keywords:

Feature extraction

Jabon

Leaf disease

Wavelet

Wavelet extraction

### ABSTRACT

Jabon (*Anthocephalus cadamba* (Roxb.) Miq) is one type of forest plants that have very rapid growth until the process of the harvest. One inhibitor is a disease that attacks the leaves in the form of spots and blight that can cause death during the growth process of this tree. The purpose of this process is to detect the object of diseases that attack the leaves of jabon at the time in the nursery. Images of affected jabon leaf disease segmented by reducing the RGB color cylinders to separate the disease object from the background. Reduced channel G-R provides information in the form of disease areas contained in the image of Jabon leaf. Furthermore, the characteristics of leaf disease can be detected well using DWT in the 3-level decomposition process with SVM classification results that can separate both classes of spots and blight by 84.672%.

*This is an open access article under the [CC BY-SA](https://creativecommons.org/licenses/by-sa/4.0/) license.*



### Corresponding Author:

Felliks Feiters Tampinongkol,  
Department of Computer Science,  
Bogor Agricultural University,  
Jl. Raya Dramaga, Dramaga Campus, Bogor 16680.  
Email: [felliks\\_ilkom2016@apps.ipb.ac.id](mailto:felliks_ilkom2016@apps.ipb.ac.id)

## 1. INTRODUCTION

Jabon (*Anthocephalus cadamba* (Roxb.) Miq) is one of the species that grow in Indonesia's forest and there are two types of Jabon plants namely red Jabon (*Anthocephalus Macrophyllus*) and white Jabon (*Anthocephalus cadamba*) both distinguishable from leaf bone color, adult leaf width (red Jabon wider than white Jabon) and the color of red Jabon tree browner [1]. Jabon is a species that trees can grow quickly, this wood can be used for the manufacture of furniture, plywood and building materials.

The cultivation and maintenance of this plant are needed to produce healthy seeds on an ongoing basis. Jabon seeding business has been done from small scale to large scale permanent nurseries. However, this effort can also find obstacles in the form of diseases of Spots and Hawar leaves that can attack the plant Jabon [2]. In the literature, the bacteria that cause leaf disease can be seen based on characteristic [3-4]. The process of making a red Jabon seedling at BPK (Balai Penelitian Kehutanan) Manado was constrained by the presence of splash and blight disease in red Jabon [5] and the technique of disease control was also performed. The process of disease identification can be done with two events, first with microscopic information that is to diagnose the type of fungus with the help of a microscope and a second macroscopic information that can explain the symptoms that arise in the host plant and can be observed directly or with the help of the camera [6]. The texture is one way that can identify the symptoms or objects contained in an image.

Texture can describe the smoothness, roughness, and regularity of an image [7]. One technique that can provide information based on the texture characteristics of an image is the discrete wavelet transform (DWT). Detection of medical images of brain regions using positron emission tomography (PET) and magnetic resonance imaging (MRI) images using DWT technique provides good accuracy [8]. Detection of blood venous sclera in the human eye using 40 eye image samples with DWT-2D feature extraction indicates a significant increase in accuracy value [9]. Automatic tea-category identification by [10] using 300 tea images using discrete wavelet packet transform (DWPT) and fuzzy SVM provides an accuracy of 97.7%. Information from feature extraction is very important to be classified based on the observed class. Based on [11] leaf disease identification based on morphology using SVM gives an accuracy value of 87.5%. The SVM classification method is capable of providing better value than the multinomial naïve Bayes classification method and the neural network (NN) to emotions in the text [12].

In this study, energy and entropy-based wavelet method used for recognize Jabon leaf diseases. An image can be decomposed into a set of sub-signals by discrete wavelet transform (DWT). The support vector machine (SVM) models used to separate leaf spots and leaf blights diseases, based on level decomposition distribution which energy and entropy wavelet method were proposed.

## 2. RESEARCH METHOD

### 2.1. Data Set

The data used are the image of red Jabon (*A Macrophyllus*) and white Jabon (*A Cadamba*) infected with the disease. The Jabon leaves observed in this study are Jabon leaves that are still in the growth process of 3-6 months of age. Data in the form of symptoms of spotting and blight on the leaves obtained from the observation process at four nursery locations nursery IPB, Pelabuhan Ratu, Cimanggis and BPK Manado. Total samples obtained 913 images of red and white Jabon leaves infected with the disease Figure 1.



Figure 1. Seeds of red Jabon (a) and Seeds of white Jabon (b)

### 2.2. Methodology

The method in this research consists of six stages including data acquisition, preprocessing, feature extraction, classification, analysis, and evaluation. The flow of the research process can be illustrated in Figure 2.

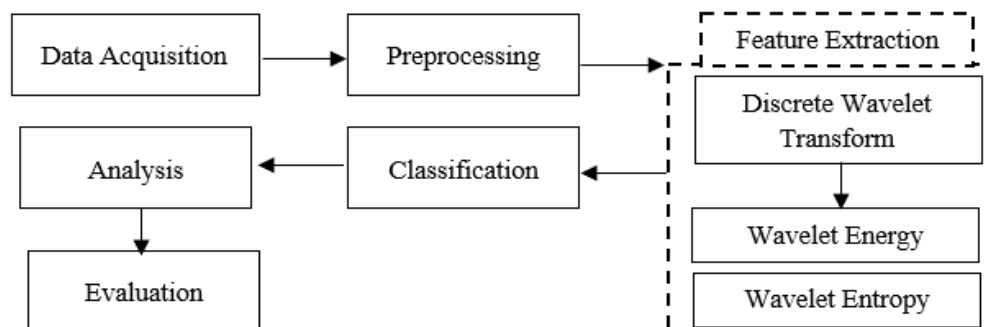


Figure 2. Flowchart diagram

### 2.2.1. Data Acquisition

Photos of red and white jabon leaf infected by the diseases taken using a digital camera, leaf position is in the middle with a white background. Total 913 images of jabon leaf with 468 images of white jabon leaf and 445 red jabon leaf. Photograph of jabon leaf is shown in Figure 3. Leaf spots are usually rather definite spots of varying sizes, shapes and colors. There is nearly always a distinctive margin. [13]. This disease is caused by the fungi *Rhizoctonia* sp [14] and is caused also by the *Colletotrichum* sp fungi [15]. Leaf blights are generally larger diseased areas than leaf spots and more irregularly shaped [16]. Sometimes the blighting appearance of leaves is the result of the coalescence of numerous small spots. The cause of this disease is by *Fusarium* sp [17].

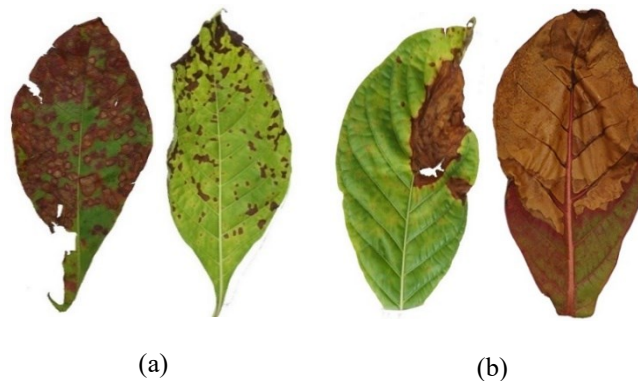


Figure 3. Leaf disease on Jabon, (a) leaf spot, (b) leaf blight

### 2.2.2. Preprocessing

The first step image of jabon leaves labeled for easy recognition and separated then the size of the image is compressed into  $\pm 300$  KB for each image to facilitate the process of computing. The image of the jabon leaf that has been labeled and compressed is then segmented using the RGB color intercept reduction technique [18]. The RGB color channel separation consists of R-G, R-B, G-R, G-B, B-G, and B-R [19]. The segmented leaf area is segmented in the reduction of green-red (G-R) channels and the healthy leaf area is segmented on the red-green channel (R-G). Channel selection depends on the information required. In the G-R channel, the segmented disease segment as white and black is a healthy leaf area Figure 4.

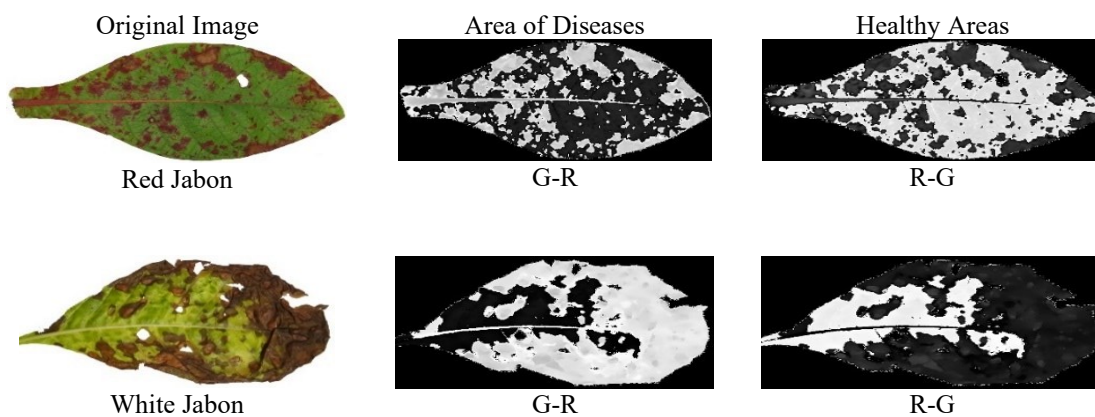


Figure 4. Segmentation Channel Red, Green, Blue (RGB)

### 2.2.3. Feature Extraction

The feature extraction technique used discrete wavelet transform (DWT) according to [20-21] wavelet is a small wave that has the ability to classify image energy and concentrated on a group of small

coefficients. Wavelet is a function that can shred data into different sets of frequencies, making it easy to learn [22]. The process of wavelet decomposition can be seen in Figure 5.  $y_{high}$  and  $y_{low}$  are a high-pass filter (HPF) and low-pass filter (LPF),  $y_{high}$  is referred to as the DWT coefficient.  $y_{high}$  is the detail of the signal information, whereas  $y_{low}$  is a crude approximation of the scaling function [23]. The information from each wavelet decomposition subgroup will be calculated using wavelet energy and Shannon entropy to serve as a feature space for prediction [24-25]. Formula feature extraction as shown in Table 1.

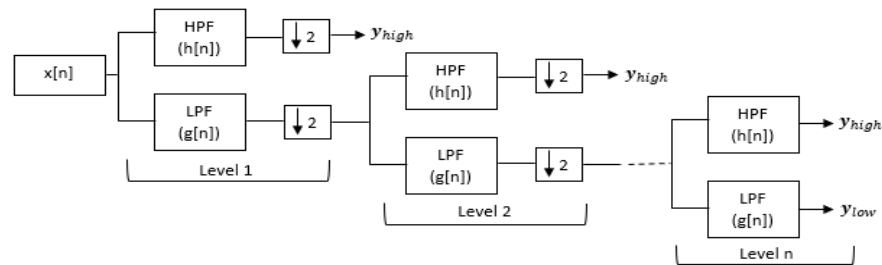


Figure 5. Wavelet discrete decomposition

Table 1. Formula feature extraction

Feature Extraction	Formula	Description
Wavelet Energy	$E_i = \sum_{n=1}^N  f(n) $	Energy for each sub-band of wavelet decomposition
	$E_{tot} = \sum_{i=1}^{2^J} E_i$	The total energy value obtained from each sub-band
	$P_i = \frac{E_i}{E_{tot}}$	Normalization of wavelet energy value
Shannon Entropy	$S = - \sum_{i=1}^N P_i \log_2(P_i)$	Provides information in the form of a random value of the wavelet decomposition spectrum

### 3. RESULTS AND ANALYSIS

The reduction of the G-R color channel is able to separate the object of the disease with the background so that in the texture feature extraction process using DWT color channel G-R is selected for the decomposition process. Decomposition is done as much as 3-level because at decomposition level-3 noise decreases and characteristic of disease becomes clearer. The classification process uses the feature values obtained from wavelet energy and entropy. The evaluation technique uses a confusion matrix.

#### 3.1. Wavelet decomposition

Wavelet decomposition process is done as much as 3-level decomposition with the result of G-R segmentation which becomes the image of input in doing the decomposition process. The higher the decomposition process the noise will decrease, so the value of disease features obtained from the calculation of wavelet energy and Shannon entropy more detail. Wavelet decomposition provides information of approximation (LL), horizontal (HL), (LH) vertical, and (HH) diagonal.

The subband has different information on the LL sub-band of information given in the form of crude approximate values of the input image. Subband LL is the result of DWT whose x-axis is converged with low pass filtering (LPF) and the y-axis is converted by high pass filtering (HPF). HL axis x is convolved with HPF and the y-axis is convolved with LPF so as to make a horizontal direction detected. The LH sub-band is an x-axis DWT process convolved with LPF and the portion on the y-axis is convolved with HPF so that vertical line is detected. HH values are obtained from the x-axis and the y-axis is convolved using HPF so that lines with diagonal direction are detected.

The process of wavelet level-1 decomposition can be seen in Figure 6 (a). The DWT decomposition process at level 2 produces 4 sub-bands LL, LH, HL, and HH just as in the previous decomposition process. However, in the process of decomposition level-2 and so on no longer use the image of segmentation results as input but the value of LL sub-band on decomposition level-1 which becomes input for further decomposition process.

The y-axis of the spectrum shows the frequency value and the x-axis shows the pixel position of the input image. Therefore, by using DWT the disease of Jabon leaf can be detected by looking at the fluctuating spectrum value in each decomposition process (a), (b) and (c). As in Figure 6 (c) the noise is decreasing so that the pixel position of the diseases of spotting and blight becomes more apparent.

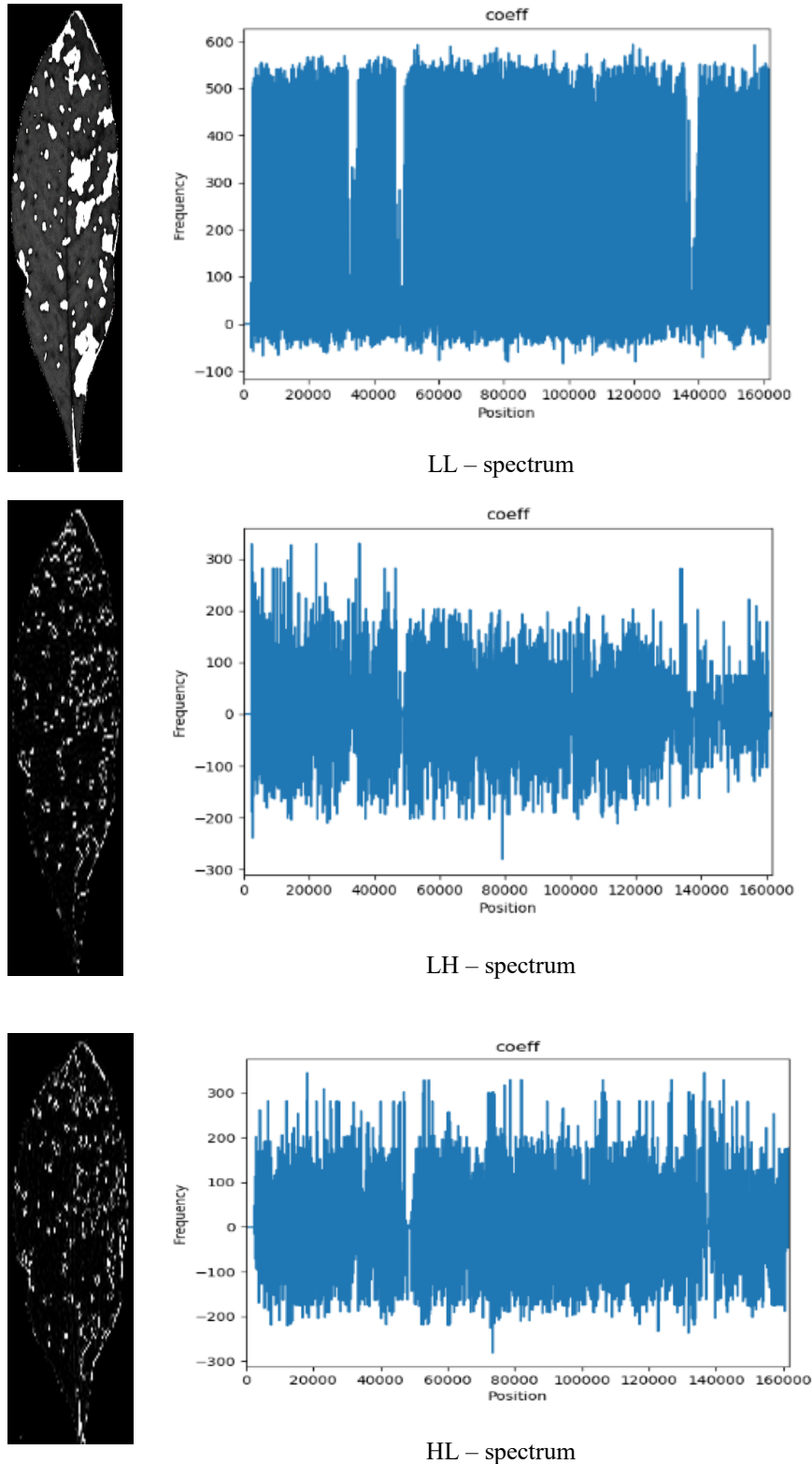


Figure 6. (a) Decomposition process level-1 (Decomposition wavelet level-1)

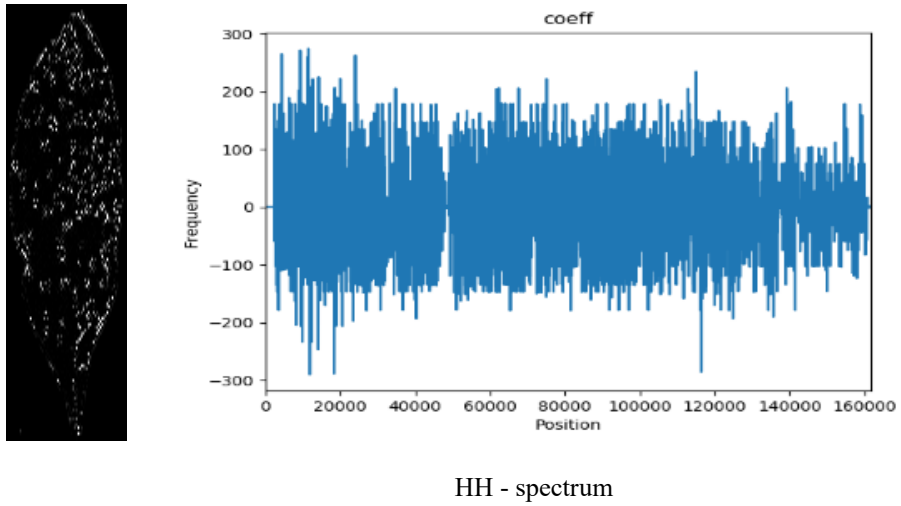


Figure 6. (a) Decomposition process level-1 Decomposition wavelet level-1 (continue)

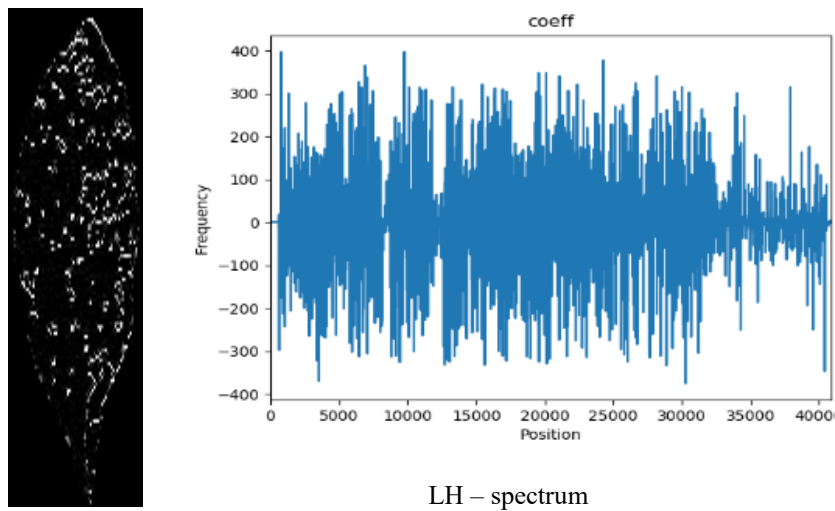
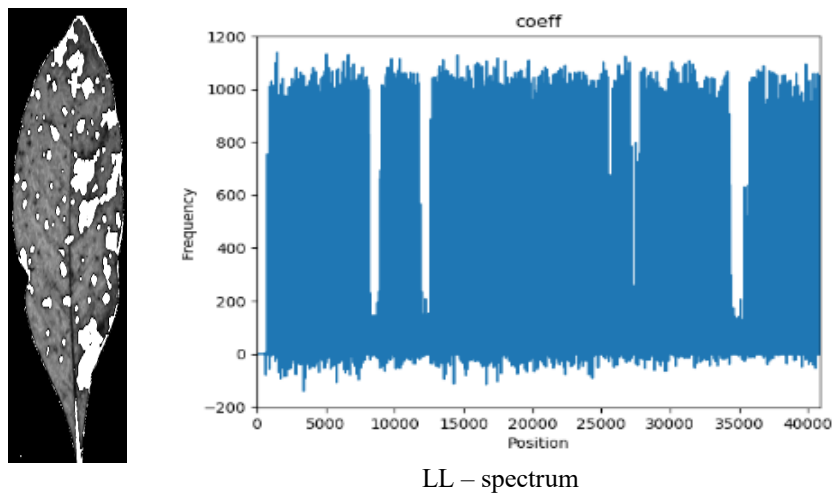
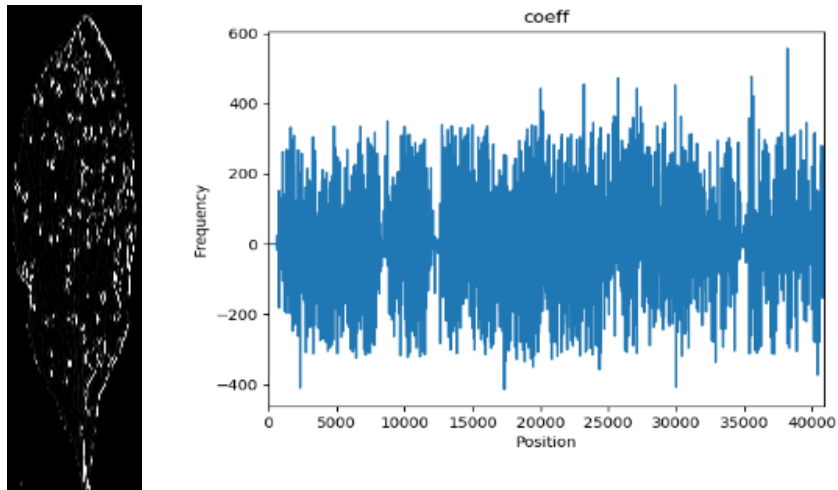
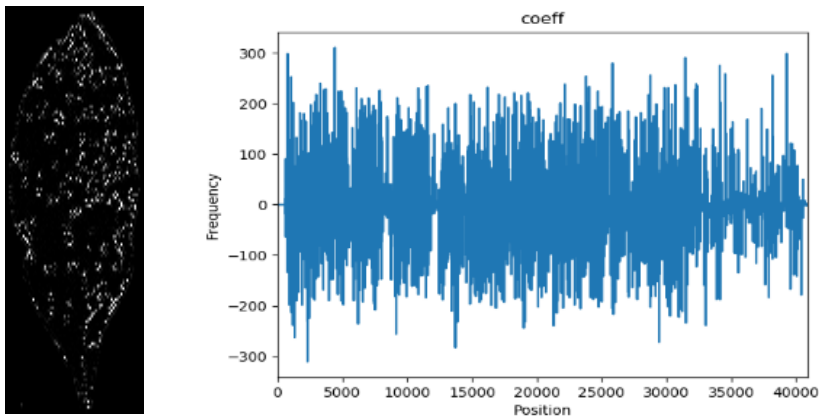


Figure 6. (b) Decomposition process level-2 (Decomposition wavelet level-2)

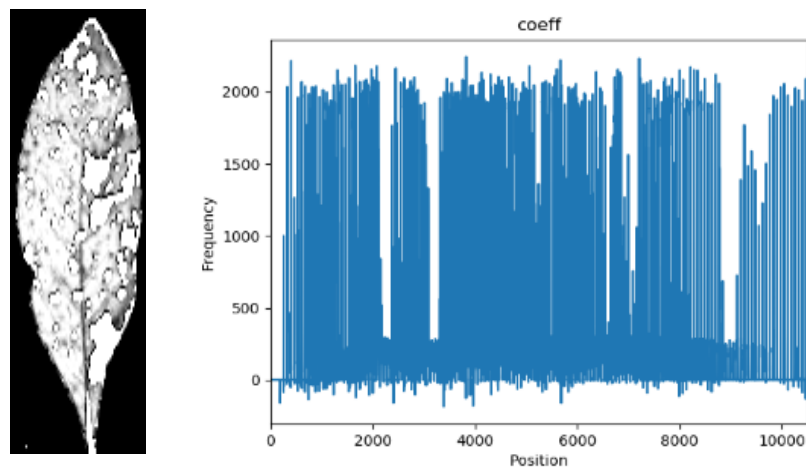


HL – spectrum



HH - spectrum

Figure 6. (b) Decomposition process level-2 (Decomposition wavelet level-2) (continue)



LL – spectrum

Figure 6. (c) Decomposition process level-3 (Wavelet level-3 decomposition)

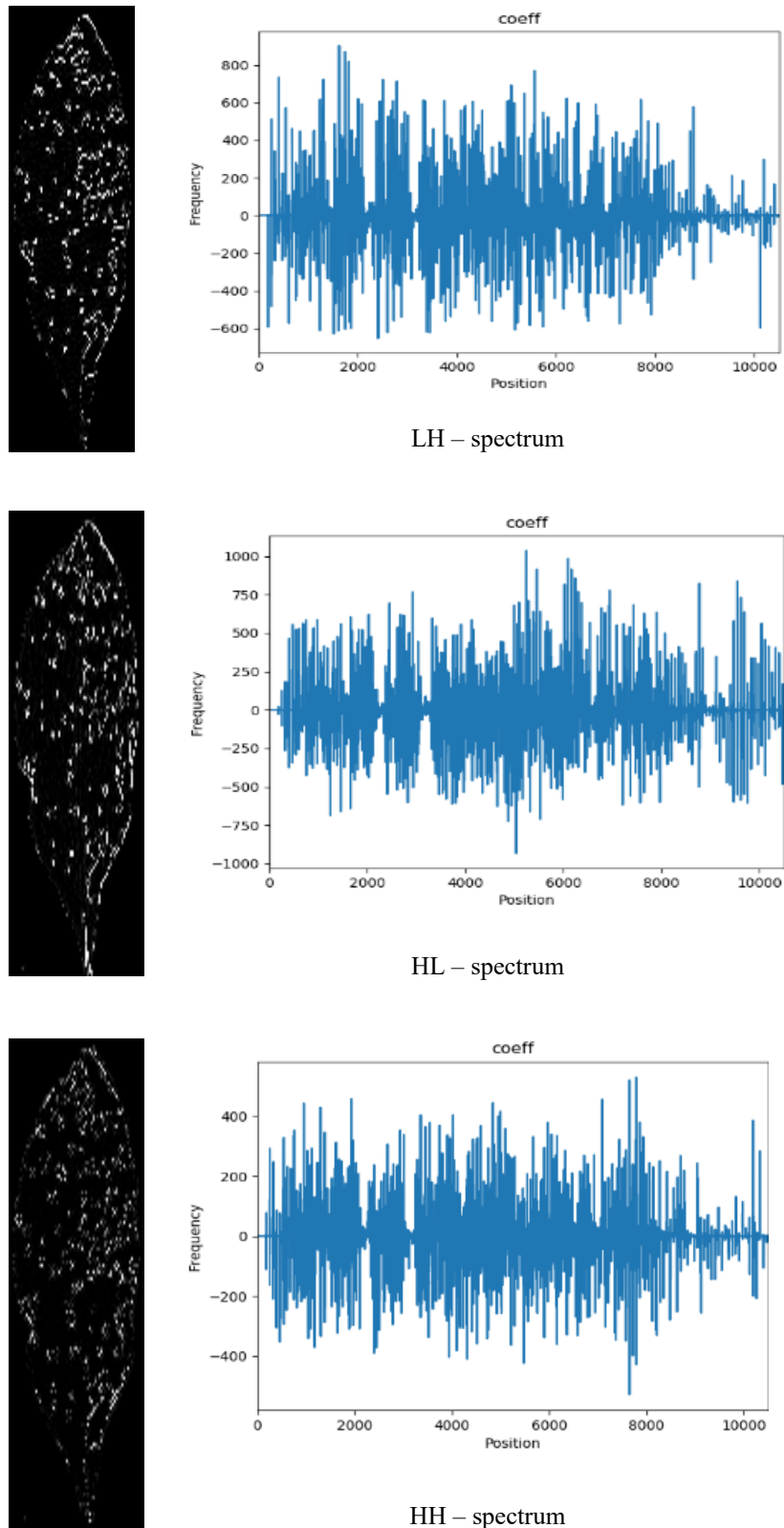


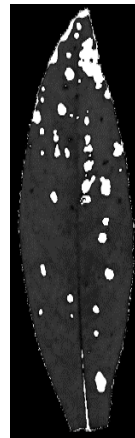
Figure 6. (c) Decomposition process level-3 (Wavelet level-3 decomposition) (continue)

### 3.2. Wavelet energy and entropy

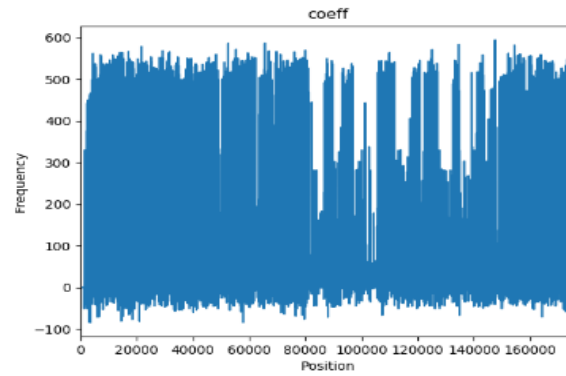
When wavelets are applied to a discrete signal, low-pass and high-pass filters are used, splitting the data into a low frequency (approximation) part and a high frequency (detail) part. The data distribution from the LL sub-band gives a high accuracy value so that the energy and entropy values of the LL will be



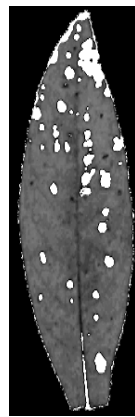
processed to build the SVM model. The energy wavelet shows the regularity value of the spectrum and entropy measures a random value based on the occurrence of the spectrum. Both of these values will be the founders to perform the classification process. The approximation energy and entropy level 1, 2 and 3 values can be seen in Figure 7.



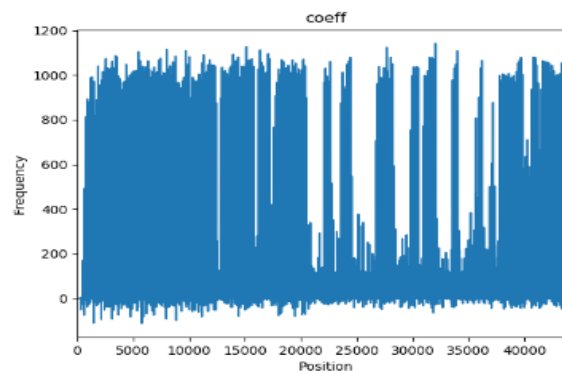
LL-1



Spectrum  
 Nilai energy: 8948533.49  
 Nilai entropy: 15.978967518



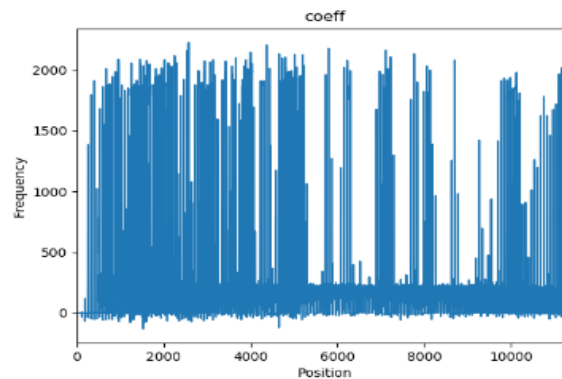
LL-2



Spectrum  
 Nilai energy: 4465997.20  
 Nilai entropy: 14.022177246



LL-3



Spectrum  
 Nilai energy: 2232297.42  
 Nilai entropy: 12.091749071

Figure 7. Energy and Shannon Entropy Value

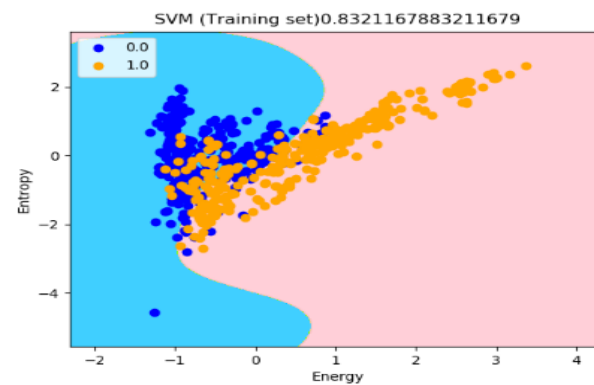
### 3.3. Classification

Table 2 provides the comparison of SVM model accuracy level according to kernel Radial Basis Function (RBF). The identifier used for classification is the energy and entropy value of each image of Jabon leaf. Distribution of data used in the classification is the distribution of energy data LL x axis and entropy LL axis y. The support vector model is obtained from comparing the 10-fold cross validation value with the resulting value of each fold.

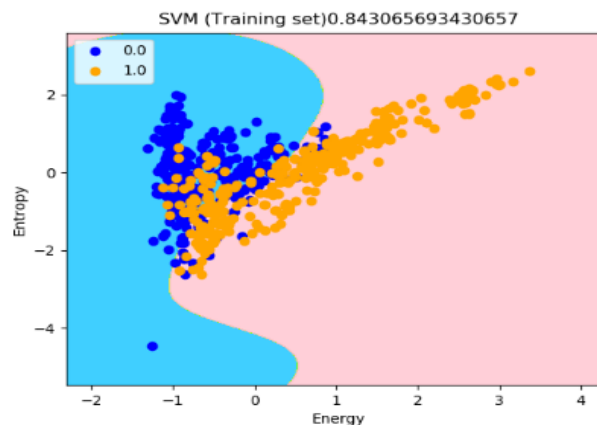
The value of the fold is close to the average value to be selected as the support vector model. Average level of accuracy of level-1 83.723%, level-2 84.270% and level-3 84.416%. Based on Table 2 the accuracy value at level-1 is close to the average value is model 3, level-2 model 3 and level-3 model 1. The highest accuracy is shown on the level-3 accuracy value 84.672% model-1. Data distribution and SVM model for each level can be seen in Figure 8.

Table 2. Support vector 10-fold cross validation models

K-fold	Accuracy Value Level-1 (%)	Accuracy Value Level-2 (%)	Accuracy Value Level-3 (%)
1	84.672%	84.672%	<b>84.672%</b>
2	85.766%	86.496%	85.036%
3	<b>83.212%</b>	<b>84.307%</b>	84.672%
4	82.482%	82.117%	83.212%
5	85.401%	86.861%	85.401%
6	84.307%	85.401%	85.401%
7	81.387%	81.752%	82.117%
8	83.212%	83.942%	85.036%
9	84.307%	84.307%	85.401%
10	82.482%	82.847%	83.212%
<b>Average</b>	<b>83.723%</b>	<b>84.270%</b>	<b>84.416%</b>

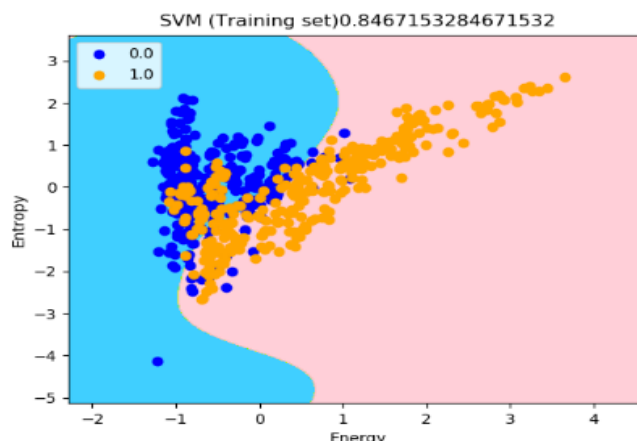


Model 3 LL level-1



Model 3 LL level-2

Figure 8. Support vector machine models



Model 1 LL level-3

Figure 8. Support vector machine models (continue)

#### 4. CONCLUSION

Reduced green-red color channel (G-R) successfully separates the disease object from the background very well although in some photos there are segmented leaf bones as illness. Feature extraction using DWT is able to provide more detailed leaf disease information at level-3 decomposition with reduced noise. The entropy and energy values obtained from the LL spectrum approximation of each decomposition level become the feature space in SVM classification. The SVM support vector machine classification model using RBF radial base function carrels provides the highest level of 3rd-level decomposition value of 84.572% with 119 spotted and 113 correctly classified blight results from 274 data test.

#### REFERENCES

- [1] Bhumakar H and Dr. Sailesh Naryan, "A Review on: Pharmacological Activity of Anthocephalus Cadamba," *World Journal of Pharmaceutical Research*, vol. 7, no. 16, pp. 383-394, 2018.
- [2] Krisnawati H, Maarit K and Markku K., "Anthocephalus cadamba Miq. Ecology, Silviculture and Productivity," *Center for International Forestry Research (CIFOR)*, Bogor, Indonesia, pp. 11, 2011
- [3] Aisah A. R., Soekarno B. and Achmad, "Pathogenicity of Botryodiplodia spp. Isolates on Jabon (Anthocephalus cadamba (Roxb.) Miq)," *Jurnal Penelitian Hutan Tanaman*, vol. 14, no. 2, pp. 85-101, December 2017.
- [4] Yunasfi, "Factors that Influence the Development of Diseases [in bahasa: Faktor-Faktor yang Mempengaruhi Perkembangan Penyakit]," Medan (ID): USU Digital Library, May 2002.
- [5] Khanzada M. A., Lodhi A. M. and Shahzad S., "Mango Dieback and Gummosis in Sindh, Pakistan Caused by Lasiodiplodia theobromae," *Plant Health Progress*, January 2004.
- [6] Streets, R. B., "Diagnosis of Plant Diseases," *University of Arizona Press; 1st edition*, pp. 245, January 1972.
- [7] Gonzalez R, Woods R., "Digital Image Processing," *Third Edition*, pp. 976, 2007.
- [8] Bhavana V., Krishnappa H. K., "Multi-Modality Medical Image Fusion – A Survey," *International Journal of Engineering Research & Technology (IJERT)*, vol. 4, no. 2, pp. 778-781, February 2015.
- [9] Tayade P. S., Neha R., "Sclera Feature Extraction using DWT Co-efficients," *2017 2nd International Conference on Communication and Electronics Systems (ICCES)*, Coimbatore, pp. 256-259, 2017.
- [10] Phillips P, Wang S, Yang J, Yang X, Yuan TF, Zhang Y., "Identification of Green, Oolong and Black Teas in China via Wavelet Packet Entropy and Fuzzy Support Vector Machine," *Entropy*, vol. 17, no. 10, pp. 6663-6683, September 2015.
- [11] Manik F. Y., Herdiyeni Y., Herliyana E. N., "Leaf Morphological Feature Extraction of Digital Image Anthocephalus Cadamba," *TELKOMNIKA*, vol. 14, no. 2, pp. 630-637, June 2016.
- [12] Azim M. A., Mahmudul H. B., "Text to Emotion Extraction Using Supervised Machine Learning Techniques," *TELKOMNIKA*, vol. 16, no. 3, pp. 1394-1401, June 2018.
- [13] Agrios G. N., "Plant Pathology," *Academic Press; fifth edition*, 2005.
- [14] Herliyana E. N., Achmad, Putra A., "Liquid Organic Fertilizer Influence on Jabon (Anthocephalus cadamba miq.) Seedling Growth and Its Resistance to Disease," *Jurnal Silviculture Tropika*, vol. 3, no. 3, December 2012.
- [15] Chandrashekar K. S. and Prasanna K. S., "Antimicrobial Activity of Anthocephalus cadamba Linn," *Journal of Chemical and Pharmaceutical Research*, vol. 1, no. 1, pp. 268-270, 2009.

- [16] Aisah A. R., Soekarno B. and Achmad, "Isolation and Identification of Fungi Associated with Dieback of Jabon Seedling (*Anthocephalus Cadamba* (Roxb.) Miq)," *Jurnal Penelitian Hutan Tanaman*, vol. 12, no. 3, pp. 153-163, December 2015.
- [17] Hanif N. H. and Anggraeni I., "Identification of Causes of Red Leaf Spot on Red Jabon (*Anthocephalus Macrophyllus* (Roxb.) Havil) Seeds In Kima Atas Permanent Nursery, Forestry Research Institute of Manado," *Jurnal Wasian*, vol. 2, no. 2, pp. 73-78, 2015.
- [18] Minichino J. and Howse J., "Learning OpenCV 3 Computer Vision with Python Second Edition," *Packt Publishing, 2 edition*, pp. 268, September 2015.
- [19] Herdiyeni Y., Muhammad IJ., Setio T., Bayo AS., "Automatic Identification of Acacia Leaf Diseases in Plantation Forests using Wavelet Energy and Shannon Entropy," *2017 International Conference on Information and Communication Technology Convergence (ICTC)*, Jeju, pp. 570-575, 2017.
- [20] Lahmiri S., "Wavelet Low- and High-Frequency Components as Features for Predicting Stock Prices with Backpropagation Neural Networks," *Journal of King Saud University-Computer and Information Sciences*, vol. 26, no. 2, pp. 218-227, July 2014.
- [21] Filters W. and Transforms W., "Preview of Wavelets, Wavelet Filters and Wavelet Transforms," *Space & Signals Technologies LLC*, pp. 1-30, 2009.
- [22] Daubechies I., "Wavelets and Other Phase Space Localization Methods," *Proceedings of the International Congress of Mathematicians. Zurich, Switzerland*, pp. 57-74, November 2000.
- [23] Tuakia N., Suprpto M., Yudistira, "Implementation of Watermarking in Medical Image using Discrete Wavelet Transform (DWT) Method," *Doro Jurnal Universitas Brawijaya Malang*, vol. 2, no. 8, pp. 63-70, 2013.
- [24] Pederiva R, Varanis M., "Wavelet Packet Energy-Entropy Feature Extraction and Principal Component Analysis for Signal Classification," *Proceeding Series of the Brazillian Society of Applied and Computational Mathematics*, vol. 3, no. 1, 2015.
- [25] Tan C., Yanping W., Zhou X., Zhongbin W., Zhang L., and Liu X., "An Integrated Denoising Method for Sensor Mixed Noise Based on Wavelet Packet Transform and Enrgy-correlation Analysis," *Journal of Sensors*, vol. 2014, pp. 11, Oct. 2014.